SLAC-PUB-1129
(ACC)
October 1972

THE SLAC RECIRCULATING LINEAR ACCELERATOR (RLA)

R. H. Helm, W. B. Herrmannsfeldt, H. A. Hogg, A. V. Lisin,
G. A. Loew, J. J. Murray, R. B. Neal, P. B. Wilson

Stanford Linear Accelerator Center
Stanford University, Stanford, California 94305

1. INTRODUCTION

Recirculation of the SLAC beam to double its energy or increase its duty cycle has been under study for the past two years. This paper is a status report on this project for which it is hoped that at least partial authorization will be granted next year. The basic concepts involved have been described in earlier papers.[1,2] The potential expansion of the SLAC physics program resulting from this project was covered elsewhere.[3]

The principle of the Recirculating Linear Accelerator (RLA) is illustrated in Fig. 1. The beam is accelerated once through the existing accelerator to a maximum energy of 20 GeV. It is then extracted and stored in the 6.9 km-long recirculator for 120 revolutions, corresponding to one machine interpulse period of 1/360 sec. Then, when the klystron system is ready for the next rf pulse, the beam is reinjected into the accelerator for a second pass. The present maximum energy of 25 GeV would thus be increased to 45 GeV by the second acceleration. Alternatively, it is possible to use the recirculator as a "beam stretcher" by spilling a fraction of the beam on each turn. Since the recirculating period is 23 μsec and the beam pulse is 1.6 μsec long, the resulting duty cycle is 7%.

The recirculator proper consists of two 95 m-radius loops located at the ends of the 3 km-long accelerator housing and joined by two long straight sections. The beam is bent around the loops by an array of 160 alternating-gradient magnets. Two 30° reverse bends are used to connect the loops to the straight sections. The reverse bends contain an array of quadrupoles and bending magnets which make it possible to adjust the isochronism of the entire recirculator to an extraordinarily low value. The long straight sections are located just above the present accelerator in the same housing. Besides the focusing and steering system, these straight sections include the rf system which makes up for synchrotron radiation losses, and the "long spill" extractor for the long duty-cycle beam.

2. BEAM DYNAMICS

2.1 Requirements

The RLA storage system consists of the two magnet loops coupled by two long straight sections each containing part of the rf system. The chief requirement on the beam dynamics of the RLA is that the 6-dimensional phase space should not grow

(Presented at the IIIrd All Union Conference for Scientific Problems of Charged Particles Accelerators, Moscow, October 2 - 4, 1972.)

to be greater than the acceptance of the accelerator during the storage interval. The acceptance of the accelerator is limited by the requirement that a low-energy beam must be accelerated through the same structure. If the high-energy and the low-energy beams are to be accelerated together, which is a requirement for 360 pps operation of the RLA, then the acceptance of the high energy beam is limited by the strength of the focusing system that will transport the low-energy beam. Extra focusing for the high energy beam alone, in the form of pulsed quadrupole lenses, can be provided, but at the cost of limiting RLA operation to 180 pps. The present focusing system for the accelerator has a matched acceptance in either the horizontal (x), or vertical (y), plane of about $A = 0.3 \times 10^{-6}\ \pi$ meter-radians at 17.5 GeV. This can be increased by adding closer-spaced quadrupole lenses, or by adding pulsed focusing, or both, perhaps to about $A = 0.6 \times 10^{-6}\ \pi$ m-rad.

The longitudinal $\delta E \delta \phi$ acceptance of the accelerator is limited by the requirement of low momentum spread after the second pass through the accelerator. A bunch length of $\pm 8^{o}$ in phase about the rf crest results in ~1% spread of energy gained, or ~0.5% final spectrum on the assumptions that the energy is doubled on the second pass, and that the energy spread of the stored beam is negligible.

2.2 Transverse Optics

The transverse phase space of the stored beam depends primarily on the horizontal quantum-induced phase space growth and on the radiation damping. To a lesser extent, it depends on the phase space of the injected beam and on the storage time. The asymptotic value of the quantum induced term depends on the square of the energy. Since the nominal storage period of 1/360th sec is not much greater than the damping period, the beam is not at its asymptotic limit and the energy dependence is somewhat greater than E^2. At a given energy then, if the emittance from the accelerator is a constant, ($\epsilon_i = 0.05 \times 10^{-6}$ m-rad has been assumed) and if the storage time is given, the horizontal phase space depends on the quantum driving term and on the horizontal damping time constant.

The quantum driving term Q depends on an integral[4] of the properties of the lattice around the complete loop. It is primarily limited by maintaining tight focusing around the loop.

The damping rates are determined by the damping partition numbers: $J_y = 1$, $J_x = 1 - D$, and $J_\epsilon = 2 + D$ (with no x-y coupling), where the damping factor, D, is almost entirely determined by an integration[4] of lattice properties in the high gradient magnets. A small change in the strengths of the gradient magnets can make a significant change in the value of D. For example, increasing the field in the main loops by 3% reduces D from approximately 0.0 to -0.5. This has the effect of providing an adjustment for the horizontal damping rate.

The problem of choosing a magnet lattice is thus reduced to the following:

1. Find the damping factor D as a function of lattice parameters.
2. Find the quantum driving term Q as a function of lattice parameters.
3. Using Q and D, find the transverse phase emittance and determine the percentage of the stored current that can be transmitted through the accelerator.
4. Find operating parameters that will permit longitudinal stability and sufficiently short bunch length.
5. Determine the practicality of constructing a magnet system with the optimum parameters as found above.

Although other combinations are still being considered, the cell that appears to be the leading choice consists of a short (2.0 meter) high gradient focusing magnet and a long (5.7 meter) low gradient defocusing magnet. The high gradient magnet has a gradient of 1.78 kG/cm at 20 GeV. The low gradient magnet has a design orbit strength of about 10 kG at 20 GeV with a gradient of 0.48 kG/cm. Naturally, the low gradient magnet can be operated at a much higher field at the design orbit and, since it is also longer, it does most of the bending. Three examples of operation using these magnets are tabulated in Table I. All three operate at the same phase shifts per cell of $\delta\nu_x = 0.304$ and $\delta\nu_y = 0.101$.

The three cases listed in Table I are, in actuality, three different settings of the same magnets. The requirement for the same dB/dx at different values of B_0 is met, in practice, by a small sextupole correction. Thus, a change in the magnet current makes the beam follow a new closed orbit, as determined by the momentum dispersion function. The differences between the three cases represent about a 3% shift in magnet current for each case.

2.3 Longitudinal Dynamics

The bunch length at the moment of reinsertion into the accelerator depends on both the lattice parameters and on the rf voltage parameters. The lattice determines the longitudinal damping rate by $J_\epsilon = 2 + D$. The lattice also influences the synchrotron oscillation period and the quantum induced phase spread by the momentum dilation parameter α, defined by $\delta\ell/L = \alpha\ \delta P/P$. Table II lists the longitudinal parameters for three typical cases of operation using the parameters of Table I. In each case it has been assumed that the peak rf voltage available is 230 MV.

The reverse bends, which are the 30° bends that join the loops to the main tunnel, provide the means for adjusting the momentum dilation. Although it is theoretically possible to make $\alpha = 0$ (isochronous) in practice second order effects will probably limit the feasible range of α to: $10^{-5} < \alpha < 10^{-4}$.

The reverse bends correct for the dilation that occurs in the main bends by providing a shorter path for the high-momentum ray. Figure 2 shows a reverse bend

layout with the high-momentum ray indicated after being dispersed in one of the 5^{o} bends. The quadrupole singlet between the 5^{o} and 10^{o} bends adjusts the amount by which the off-momentum ray crosses the central trajectory and thus adjusts the dilation correction. The singlet in the middle is adjusted to make the system symmetric. The reverse bends themselves contribute significantly to the quantum driving term that causes both transverse and longitudinal phase space growth. The contribution is greater if the dilation correction is greater. Therefore it is advantageous to control the dilation in other parts of the loop so as to require the least amount of dilation correction in the reverse bends.

2.4 Operating Parameters

The best total transmission will probably be achieved by operating at a setting somewhere between case 2 and case 3. Here the transmission through the accelerator on the second pass is greater than 90%. If it is desired to push to the highest possible energy (near the no-load limit), then the system could be operated closer to the setting of case 1. Here the magnet current would be about 3% lower, and the transmission on the second pass would be about 80%. However, there would be less synchrotron radiation and somewhat less peak rf voltage would be required, thus permitting higher maximum stored energy.

3. BEAM STRETCHER

The "beam stretcher" or "long spill" system consists of a slow extraction deflector and a suitable system for transporting the beam into the switchyard. One type of extraction system being studied is based on a stochastic (Coulomb scattering) method similar in some respects to methods considered at NAL[5] and CERN.[6] An alternative system being investigated is a nonlinear magnetic perturbation method. Computer simulation studies of many versions of both methods indicate that a satisfactory slow spill can probably be obtained using either method. Results calculated for the magnetic method indicate $\gtrsim$95% extraction efficiency for a septum thickness equal to 1% of the initial beam diameter. Losses are mainly incurred on the septum with minor losses on the pipe walls in the vicinity of the perturbation. For the stochastic method the highest calculated efficiencies are $\lesssim$ 95% with comparable losses on the septum and on apertures in the recirculator. The latter result from enlarged phase areas caused by the Coulomb scattering.

A satisfactory magnetic perturbation is the field produced by a pair of conductors carrying equal and opposite currents running parallel to the electron beam axis and separated vertically by a distance somewhat less than the initial beam diameter (a bifilar loop) as shown in Fig. 3. The basic idea is to sweep the electron beam horizontally toward the perturbation at a controlled rate. On each turn of the beam

around the recirculator the perturbation deflects a small part of the beam, mainly in the vertical plane, and sends that part past a thin septum of a d.c. electrostatic deflector and into a long spill extraction channel. The remainder of the beam is sent symmetrically through an identical but cancelling perturbation and reenters the recirculator "unperturbed". The process continues until all of the beam is finally ejected. The spill rate may be controlled more or less arbitrarily by controlling the horizontal deflection rate. It turns out that a uniform deflection rate gives a nearly uniform spill rate.

4. INSTABILITIES

A number of known incoherent and coherent instabilities could lead to beam loss or deterioration of beam quality, and will have to be taken into account in RLA operation. Some of these are:

Synchrotron quantum fluctuation — which drives incoherent growth in both horizontal and longitudinal phase space. This effect has been discussed in Section 2.3.

Structure resonances — characteristic of circular machines. The strong linear integer and half-integer resonances must be avoided by proper choice of tune; the values of ν_x and ν_y can be set independently by rather small adjustments of the quadrupoles. The third-integer resonances may also be rather strong because of sextupole corrections which are required for control of chromaticity. It seems unlikely that nonlinear resonances higher than third or fourth integral will be strong enough to drive significant beam growth during the rather short (2.8 msec) storage time.

Transverse cumulative (SLAC-type) beam breakup — which arises from a coupling impedance between the beam and an rf deflecting mode in the accelerating structure. The two passes through the accelerator and the 120 passes through the recirculator linac all contribute to the deflection. Preliminary estimates indicate that the breakup threshold will be no lower than 20 to 30 mA and can be raised if necessary by increasing the focusing in the recirculator linac.

Longitudinal cumulative beam breakup — analogous to the transverse type mentioned above. The coupling impedance for this mechanism, as proposed by M. Sands, is provided by the recirculator linac. Analysis shows that there must be an error of the correct sign between the beam bunching frequency and the linac synchronous frequency, in order to produce an instability; hence the effect if observed could probably be tuned out by adjusting the linac temperature. However, preliminary estimates seem to indicate current thresholds of at least several hundred milliamperes even under the worst conditions.

"Two-beam breakup" — in 360 pps operation, a low-energy beam and a high energy beam would be accelerated through the main accelerator simultaneously.

Transverse modulation of the beam would be retained during the storage period, so that the reinjected high energy beam could drive the low energy beam, and the modulation would be further amplified by the BBU interaction. The effect would thus be cumulative over many machine pulses. This mechanism has not been investigated in detail yet. There is a possibility that 360 pps operation might be limited in maximum current if damping mechanisms (synchrotron and Landau) are not sufficiently effective.

Resistive wall interactions — can cause both transverse and longitudinal instabilities. This mechanism has not been analyzed explicitly for RLA, but is expected to be much weaker than interactions which involve high Q structures such as linacs and cavities.

Other beam-structure couplings — may arise from structure discontinuities, beam monitors and so on. The proposed microwave position monitors, especially, will have to be analyzed carefully for possible coupling impedances.

RF noise and phase jitter — in the recirculator linac can lead to stochastic growth of longitudinal oscillations. Tolerances on pulse-to-pulse jitter have been estimated as a few degrees of rms phase jitter and a few percent of rms amplitude jitter. Very short-period noise, leading to bunch-to-bunch phase error within the beam pulse, probably will not be important during the short 2.8 msec storage time.

Residual gas effects — The vacuum requirement imposed by gas scattering has been estimated as $\sim 10^{-6}$ torr for a beam loss of ~1% or less. Various mechanisms have been proposed in which the beam might couple with ions from residual gas to produce instabilities. It is not considered likely that such effects will be important, but if they do occur the vacuum requirement might have to be tightened.

5. THE RF SYSTEM

As shown in Fig. 1, energy lost by synchrotron radiation is restored by auxiliary accelerator sections which are in the straight sections of the RLA loop. The energy contribution of the auxiliary accelerator must be sufficient to store a low current beam of ~20 GeV. The beam-loading characteristic must be such that a reasonable current of 20 to 30 mA peak can be stored at ~17.5 GeV. The load-line diagram of Fig. 4 shows the peak recirculated beam current as a function of recirculation energy for three alternative rf systems. Load-line A applies to two sectors (193 m) of accelerator, powered by 16 klystrons, each producing 220 kW of peak power, 24 kW average. It is seen that the maximum energy capability is about 18 GeV. Line B applies to 3 sectors (289 m) powered by 24 klystrons rated at 220 kW each. System C is for two sectors, just as in system A, but the klystron peak power has been increased to 500 kW. System C is preferred, as it allows somewhat more current at each energy than B, and is expected to be less expensive.

Standard SLAC 3 meter-long constant-gradient accelerator sections are to be used. They are arranged so that four sections are driven by each klystron. Successive groups, or "girders" of four sections are aligned alternately in the westbound and eastbound beam lines. This arrangement allows a 12 m drift pipe in between each girder, into which additional beam focusing and monitoring equipment can be inserted if required.

The drive system is installed in available space alongside existing equipment in the klystron gallery. The components of the drive system are shown in greatly simplified form in Fig. 5. The system starts with the 476 MHz signal from the master oscillator on the main drive line. Power coupled out of the existing varactor multiplier is modulated to produce a train of pulse-pairs. Each of the pulses is 2.5 μsec long, and leading edges of the pulses in each pair are separated by approximately 6 μsec (the time required for the beam to traverse the East Loop). The pulse-pair repetition rate is 43.5 kHz; i.e., the inverse of the loop circulation time, 23 μsec. The pulses are amplified to 500 W peak for distribution through a coaxial sub-drive line to the recirculator klystrons, K_R. Klystrons in the eastbound beam accelerator are pulsed to amplify the leading rf pulse in each pair; klystrons in the westbound beam accelerator amplify the delayed pulses. A nonaccelerate pulse timing is available to each klystron for phasing and maintenance purposes by merely pulsing on the "wrong" pulse.

Klystron phasing is accomplished by coupling the RLA accelerator to the automatic equipment already installed for phasing the main accelerator. Although different in detail, the logic of the phasing method[7] is unchanged. A system for beam loading compensation which changes the phase of the rf drive during the pulse appears to be the most promising of the techniques that have been studied.

6. BEAM POSITION MONITORS

The beam position monitor being developed for RLA takes advantage of the fact that the recirculating beam is bunched at 2856 MHz. Referring to Fig. 6, it is seen that the bunched beam passes through two apertured waveguides placed together in the form of a cross. The bunches induce time-varying electromagnetic fields in each waveguide, which propagate outward, predominantly in the TE_{10} mode, to matched waveguide-to-coaxial line transitions, symmetrically placed as shown.

When the beam is on-axis the phases of the output signals at opposite ends of either arm are the same. A beam-displacement δs in the x or y direction results in a differential phase shift $\delta\phi = (4\pi\delta s)/\lambda_g$, where λ_g is the effective guide wavelength modified by the presence of the aperture.

Differential phase shift information is transformed into an analog position signal by a 15 MHz I.F. phase detector circuit. Limiter amplifiers in the I.F. circuit

make the position signal independent of beam current over a range of 50 μA to 50 mA. The output is about 700 mV/mm beam displacement. About 150 monitors will be required for RLA.

7. MAGNETS

The main loops will be made up of 5^{o} cells, each containing a focusing and a defocusing magnet. Four zero-gradient magnets will match the loops to the adjacent straight sections. Short diagonal beam runs and 30^{o} reverse bends will connect each loop to the long straight beam runs in the existing accelerator housing. Twenty-four zero-gradient, $1\text{-}1/4^{o}$ bend magnets make up each reverse bend. Approximately 100 quadrupole lenses of various types will be required for all the matching and long drift lines.

In addition, there will be a number of special magnets, including three septum magnets and two fast kicker magnets, to inflect the accelerator beam into the recirculator, to reinsert the beam into the accelerator, and for the "long spill" system.

A magnet design and development program is underway using the computer program POISSON.[8] A 0.7 meter-long computer-designed magnetic model of the focusing magnet is currently being fabricated. The model will help to evaluate fabrication techniques and measurement methods.

8. VACUUM SYSTEM

The design of the vacuum system is straightforward except for the uncertain outgassing rate of the vacuum chamber walls due to synchrotron radiation. The chambers are designed for an ultimate limit of about 1 kW/meter of synchrotron radiation.

The system is designed to maintain an average pressure of 5×10^{-7} torr during beam storage. The vacuum chamber will be made of aluminum in the curved sections and of stainless steel in the straight sections. The aluminum chamber will be extruded and will have a cross section which closely conforms to the AG magnet pole shape. Approximately 150 small ion pumps ($\approx$ 9 liters/sec each) will be used to pump RLA. One pump will be located in each cell of the main loops.

Tests to determine the most economical cleaning process for the straight stainless steel sections indicate that degreasing, steam cleaning, and air baking yield outgassing rates which are as low as those attainable after chemical cleaning and vacuum baking. A further test has confirmed that a pump spacing of 100 meters is adequate in the straight sections.

9. SUPPORT AND ALIGNMENT

Supports must be provided for the magnets in the loops at the ends of the

recirculator and for the beam transport pipes and accelerator sections in the accelerator housing. Other devices such as beam monitors, collimators, and steering dipoles must also be supported at various positions in the loop. The problem of supporting components in the bends is complicated by the fact that the plane of both loops is tilted with respect to the horizontal by 4%.

The beam transport pipes in the accelerator housing will be 6.3 cm OD stainless steel tubes. They are located above the accelerator and are supported from the existing 12 m-long accelerator support girders at 6 m intervals.

Bending magnets and quadrupoles in the loop and diagonal tunnels will be supported from the ceiling as shown in Fig. 7. Horizontal and vertical adjustments will be made by means of the threaded support rods. Alignment of the transport elements in the loops will be accomplished by precision surveying techniques. External fiducials will be accurately located with respect to the centerlines of the various devices prior to installation.

ACKNOWLEDGMENT

The authors are pleased to have this opportunity to acknowledge the enthusiastic participation of many of their colleagues, especially L. Brown and W. Brunk for magnet design and K. Mallory, J. Lebacqz, and C. Olson for the instrumentation and rf systems. A number of individuals have contributed to the beam dynamics studies, but particular mention is due Helmut Wiedemann, Matt Allen and John Rees. Finally they are especially grateful for the contributions made by Matt Sands this past summer.

REFERENCES

1. R. H. Miller, R. H. Helm, W. B. Herrmannsfeldt, G. A. Loew, R. B. Neal, C. W. Olson and J. R. Rees, "Recent ideas on upgrading the SLAC accelerator," 1971 Particle Accelerator Conference, Chicago, Illinois, March 1-3, 1971.
2. W. B. Herrmannsfeldt, M. A. Allen, R. H. Helm, G. A. Loew, R. B. Neal and P. B. Wilson, "Recirculation of the SLAC beam," Proceedings of the 8th International Conference on High Energy Accelerators, CERN 1971.
3. SLAC-139, "The recirculating linear accelerator," SLAC, Stanford, California.
4. M. Sands, "The physics of electron storage rings — an introduction," Proceedings of the International School of Physics "Enrico Fermi, Course XLVI, editor B. Toushek (Academic Press, 1971).
5. A. Maschke, private communication.
6. C. Steinbach, "Slow extraction of target scattering," CERN/MPS/C070-7, 1970.
7. The Stanford Two-Mile Accelerator, R. B. Neal, ed., Chapter 12, pp. 383-409.
8. K. Halbach, private communication.

TABLE I

Lattice Characteristics at 20 GeV

Case†	Magnet Parameters				System Parameters			
	Magnet	Bend (deg)	B_0 (kG)	dB/dx (kG/cm)	D	τ_x (msec)	T_3* (%)	T_6* (%)
1	Focus	.7	4.08	1.78	-.07	4.0	80	96
	Defocus	4.3	8.82	-.48				
2	Focus	0.4	2.33	1.78	-.78	2.23	90	99
	Defocus	4.6	9.43	-.48				
3	Focus	0	quadrupole	1.78	-1.48	1.41	96	99.9
	Defocus	5.0	10.24	-.48				

TABLE II

Typical Operation With V_{rf} = 230 MV

Case†	P_0 (GeV/c)	α	I (mA)	ϕ_s (deg)	Q_s (turns)	$\sigma_\phi(T)$ (deg)	T_q/T	T_3* (%)
1	20	10^{-5}	2	20	50	3.6	10^7	80
2	19	10^{-5}	15	20	45	4.3	10^2	93
3	17.5	10^{-4}	20	35	12	8.9	10	99

*Transmission T_3 represents an accelerator acceptance of 0.3×10^{-6} π m-rad and T_6 represents an acceptance of 0.6×10^{-6} π m-rad. The transmission calculations assume typical contributions to the quantum driving term from other segments of the RLA.

†The three cases in each table refer to the same parameters, respectively.

P_0 is the momentum of the equilibrium orbit.

α is momentum dilation factor defined by $\delta\ell/L = \alpha\, \delta P/P$.

I is the maximum current that can be recirculated with the listed parameters. It is not necessarily the maximum current at the listed P_0.

ϕ_s is the phase angle measured from the rf crest.

Q_s is the number of turns per synchrotron phase oscillation.

$\sigma_\phi(T)$ is the standard deviation of phase length of a bunch at the moment of insertion.

T_q/T is the number of quantum lifetimes per storage period.

τ_x is the horizontal damping period.

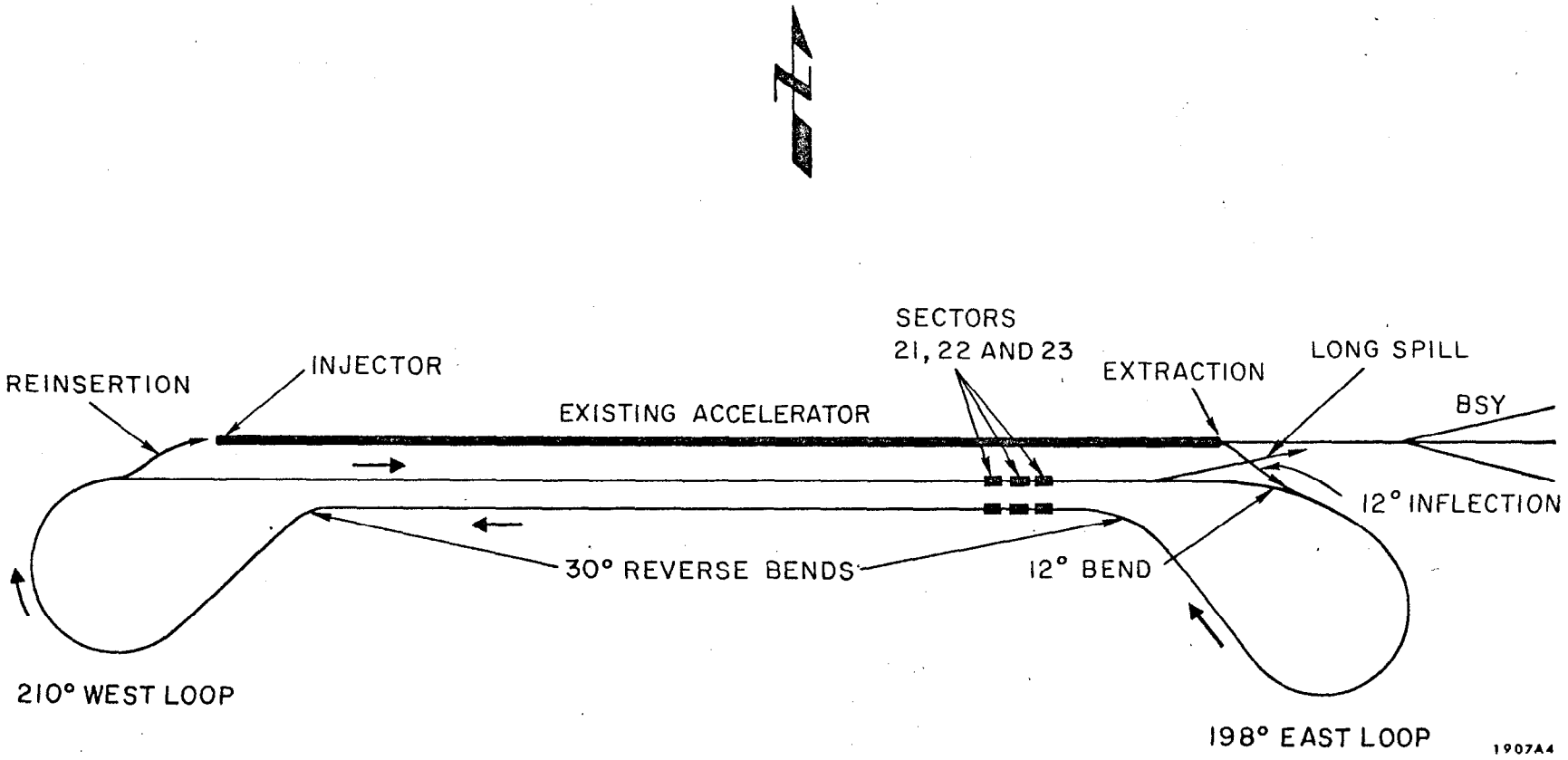

FIG. 1--Schematic layout of the recirculating linear accelerator.

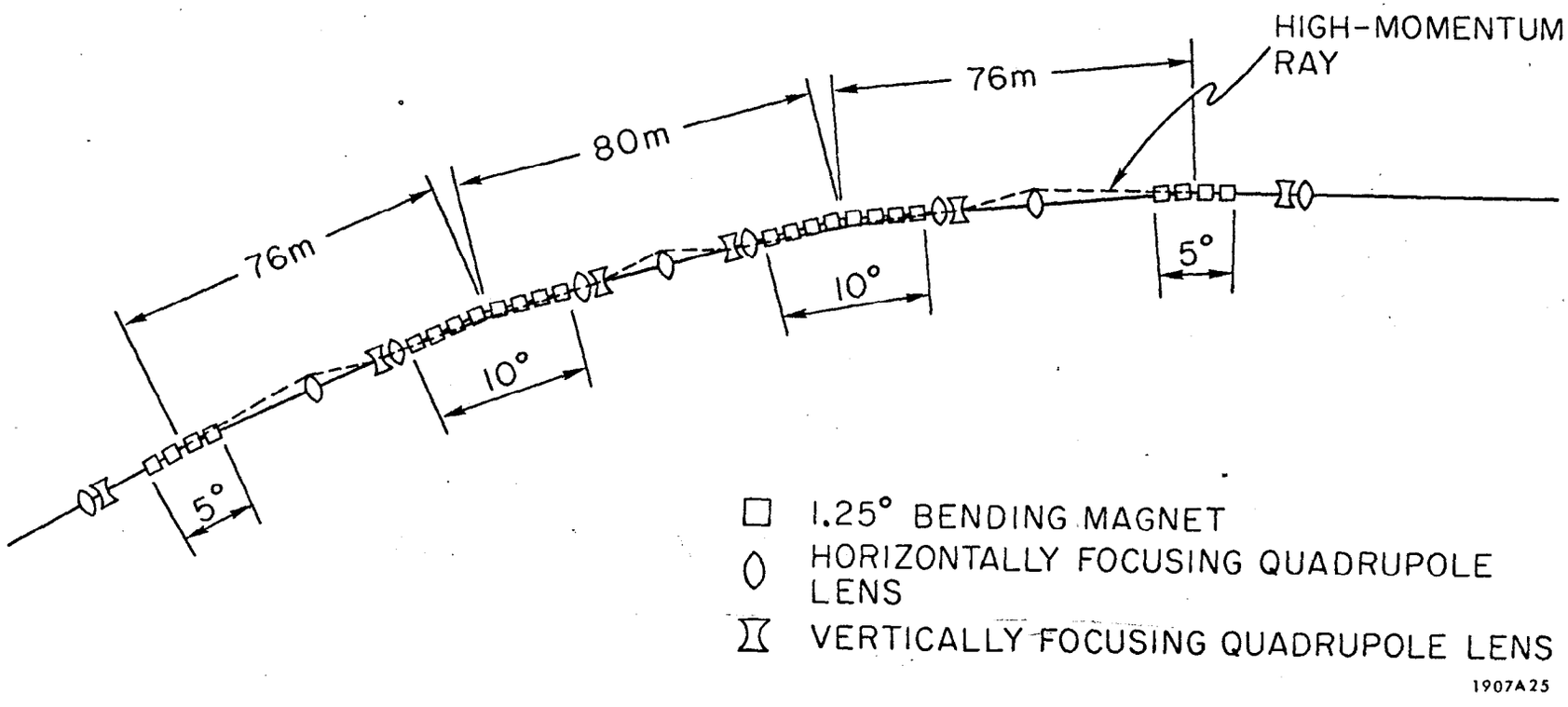

FIG. 2--Reverse bend system showing a dispersed off-momentum ray.

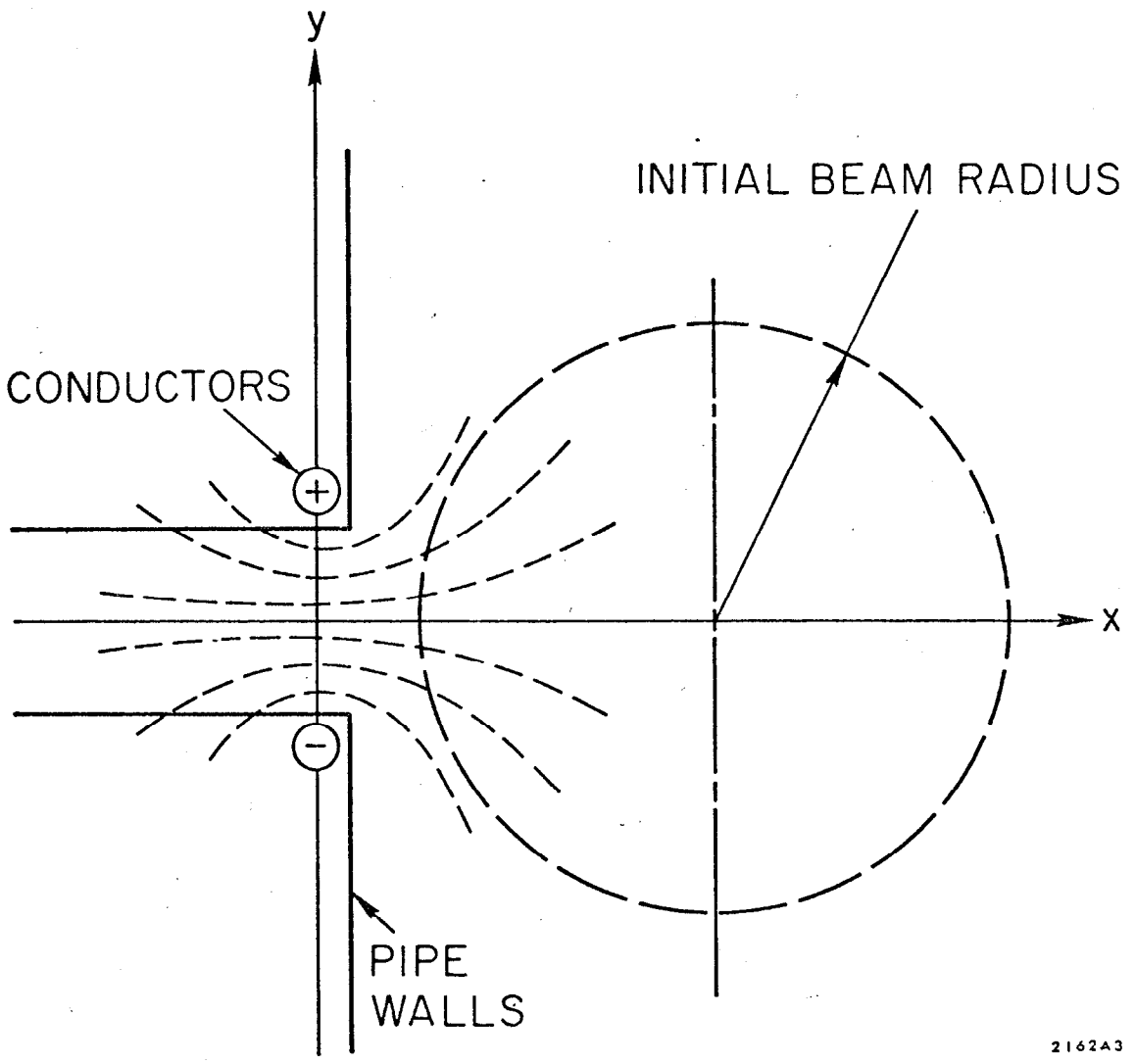

FIG. 3--Bifilar loop for magnetic perturbation suitable for a long spill extraction device.

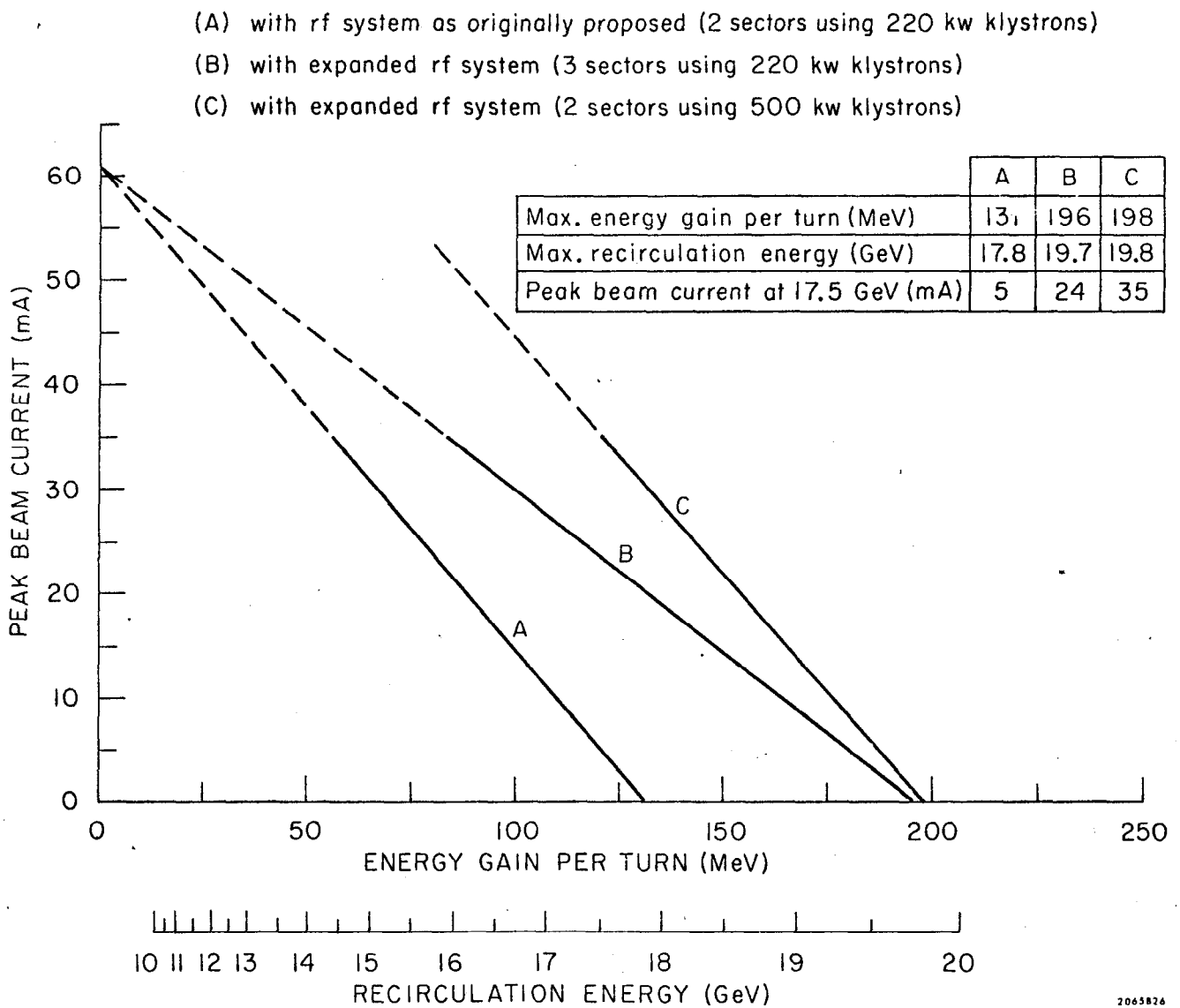

FIG. 4--Load-line diagrams comparing three different rf systems. System parameters are similar to those given for case 1 in Tables I and II at a phase angle of 30^{o}.

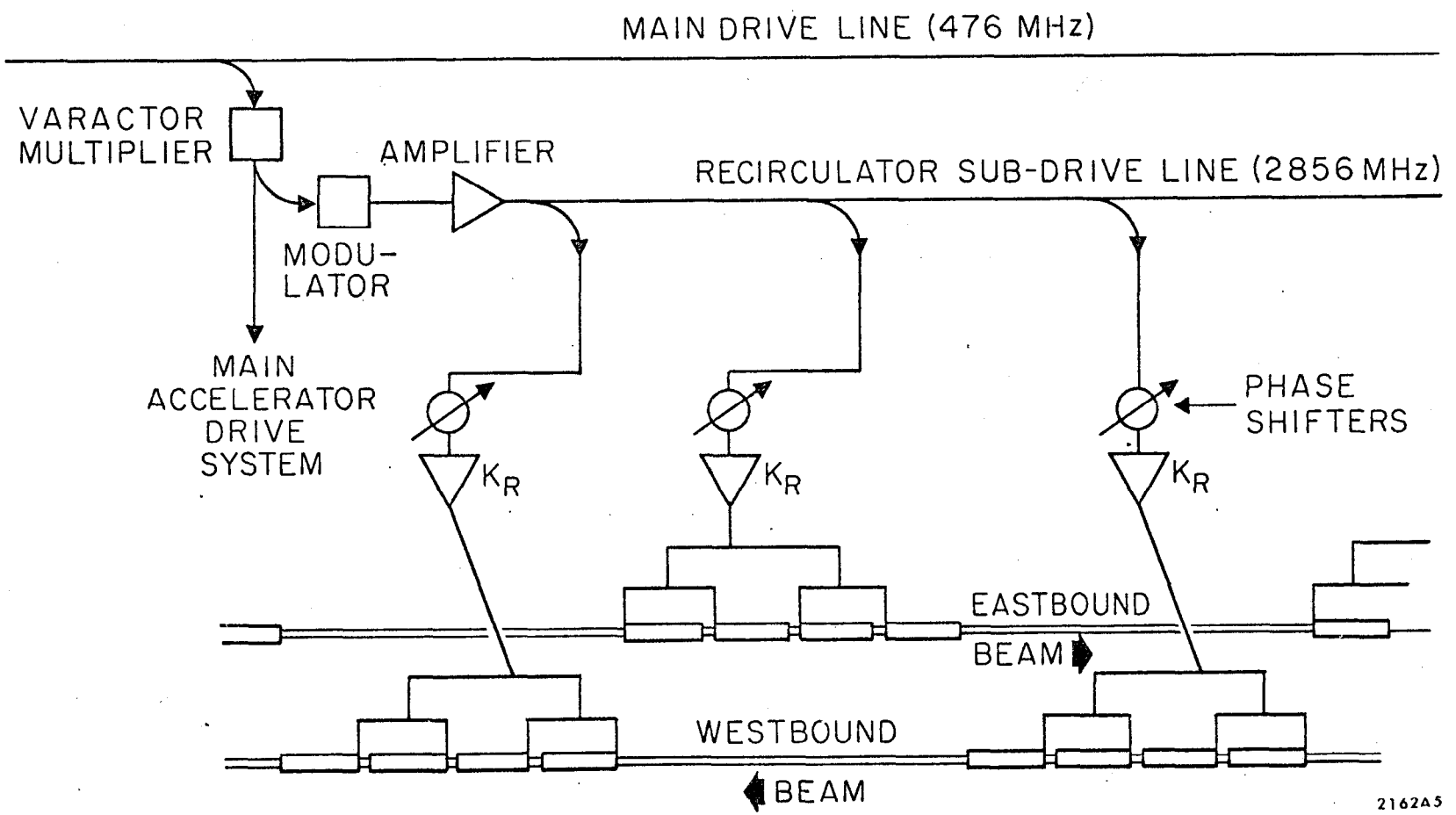

FIG. 5--Schematic of the rf drive system.

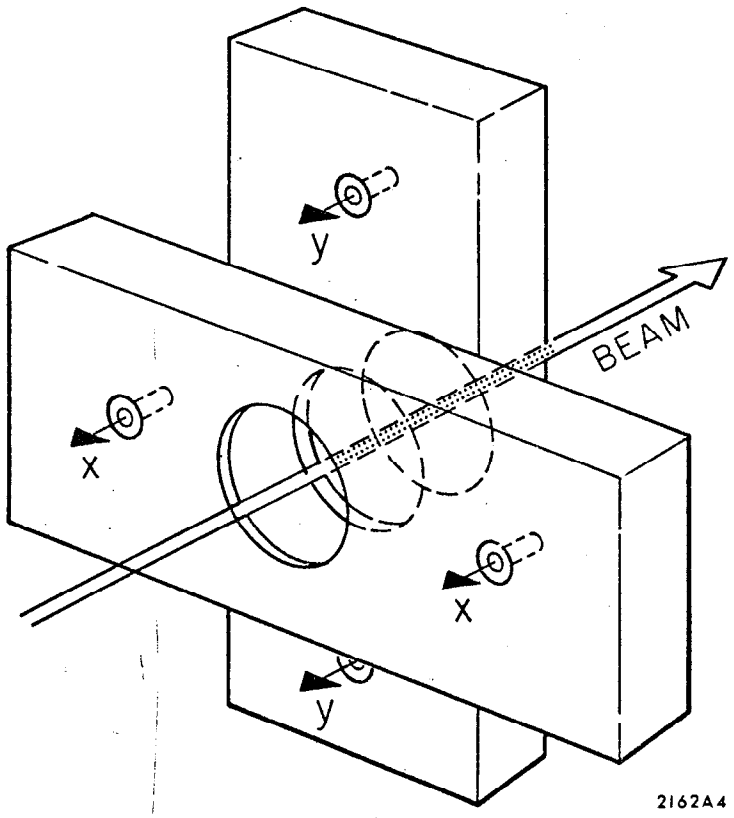

FIG. 6--Microwave beam position monitor.

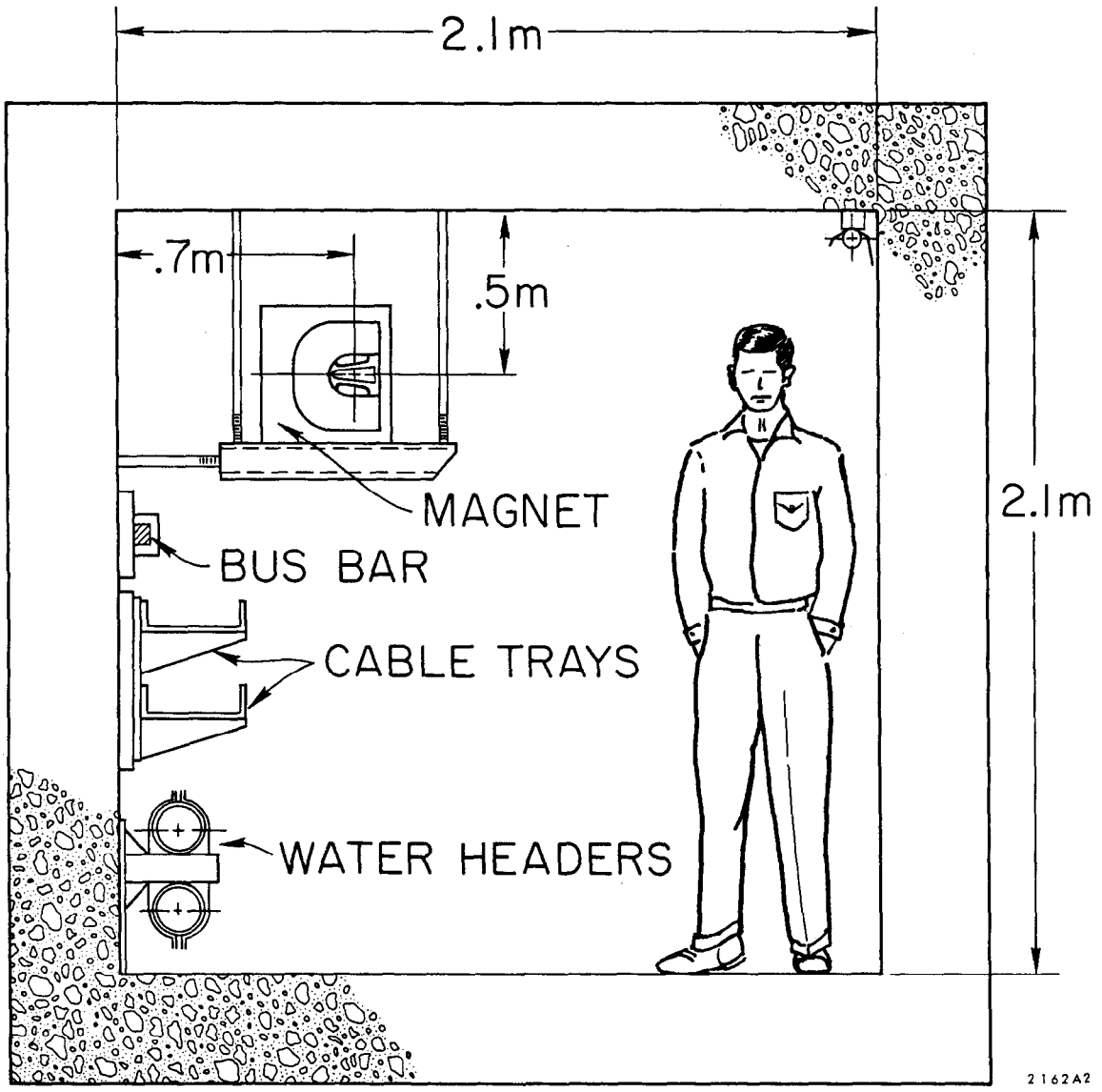

FIG. 7--Cross section of a magnet loop housing.